atmosphere

Article

Spatial–Temporal Variation and the Influencing Factors of NO_2 Column Concentration in the Plateau Mountains of Southwest China

Fei Dong [1,2], Zhongfa Zhou [1,2,3,4,*], Denghong Huang [1,2], Xiandan Du [3,4] and Shuanglong Du [1,2]

1 School of Karst Science, Guizhou Normal University, Guiyang 550001, China; 232100170578@gznu.edu.cn (F.D.); hdh@gznu.edu.cn (D.H.); 222100170570@gznu.edu.cn (S.D.)
2 State Engineering Technology Institute for Karst Desertification Control, Guiyang 550001, China
3 The State Key Laboratory Incubation Base for Karst Mountain Ecology Environment of Guizhou Province, Guiyang 550025, China; dxd@gznu.edu.cn
4 School of Geography & Environmental Science, Guizhou Normal University, Guiyang 550001, China
* Correspondence: fa6897@gznu.edu.cn

Abstract: Given the complex terrain and economic development status of Guizhou Province, research on tropospheric NO_2 column concentration using satellite remote sensing is still insufficient. Observing the spatial–temporal evolution characteristics of tropospheric NO_2 column concentration can ensure the stable development of air quality. Based on the Google Earth Engine (GEE) platform, NO_2 column concentration data retrieved from Sentinel-5P TROPOMI were analyzed using spatial autocorrelation, hotspot analysis, and geographic detector methods (Geodetector). The results show that NO_2 column concentration in Guizhou Province exhibits seasonal variation, characterized by higher levels in winter and lower levels in summer, with transitional values in spring and autumn. The annual average concentration was highest in 2021 at 3.47×10^{-5} mol/m^2 and lowest in 2022 at 2.85×10^{-5} mol/m^2. Spatially, NO_2 column concentration displays a distribution pattern of “high in the west, low in the east; high in the north, low in the south”, with significant spatial clustering. The distribution of cold and hot spots aligns with areas of high and low values. NO_2 column concentration is primarily influenced by socio-economic factors, with the interaction between any two factors enhancing the explanatory power of individual factors on NO_2 column concentration.

Keywords: NO_2 column concentration; Sentinel-5P; spatial–temporal variation; geographical detector model; Guizhou Province

Citation: Dong, F.; Zhou, Z.; Huang, D.; Du, X.; Du, S. Spatial–Temporal Variation and the Influencing Factors of NO_2 Column Concentration in the Plateau Mountains of Southwest China. *Atmosphere* **2024**, *15*, 1263. https://doi.org/10.3390/atmos15111263

Academic Editor: Yunhua Chang

Received: 23 September 2024
Revised: 12 October 2024
Accepted: 15 October 2024
Published: 22 October 2024

1. Introduction

Nitrogen oxides (NO_X), one of the six primary pollutants in the tropospheric atmosphere, are significant precursors of $PM_{2.5}$ and ozone pollution [1–4]. They primarily occur in the forms of NO and NO_2, with NO being readily oxidized to NO_2 in the atmosphere [5–7]. Currently, numerous researchers use NO_2 concentration as a proxy for NO_X levels [8,9]. As an air pollutant, NO_2 not only contributes to the formation of O_3 and other photochemical secondary pollutants but also plays a major role in acid rain, acid fog, and photochemical smog. Moreover, nitrate aerosols derived from NO_2 have considerable radiative forcing, making NO_2 a critical factor impacting climate change [10,11]. Additionally, NO_2 indirectly damages the ozone layer, affecting the ecological environment [12–14].

Situated in the eastern part of the Yunnan-Guizhou Plateau, Guizhou Province features intricate topography and fluctuating meteorological conditions that affect the inter-monthly and seasonal variations in NO_2 column concentration. The prevalent cloudy and foggy conditions lead to radiation inversion and hindered convection, thereby limiting the dispersal of pollutants such as NO_2 in the troposphere and resulting in a non-uniform spatial distribution. Consequently, the spatial–temporal distribution of tropospheric NO_2 column concentration in highland areas is intricate [15]. Although Guizhou Province is often listed among the top Chinese provinces for air quality [16,17], its role as a comprehensive reform pilot zone for Western Development, a digital economy innovation zone, an inland open economic land, and a leader in ecological civilization construction has led to industrial clustering and swift economic growth, which has affected the environment. In light of this, the suggestions of the Guizhou Provincial Committee of the Communist Party of China for drafting the 14th Five-Year Plan for National Economic and Social Development and the long-term objectives for 2035, along with the State Council's views on supporting Guizhou in pioneering a new path in the grand development of the western region (Document No. 2 of 2022) [18], stress that the green ecological development target should ensure an excellent air quality days ratio exceeding 95% in cities at or above the county level. This underscores the need to intensify efforts against pollution. In this scenario, as Guizhou continues to develop economically, it must prevent a substantial increase in NO_2 concentration, making the province's atmospheric environmental status and pollution control a matter of significant concern [19].

In recent years, remote sensing technology has increasingly become a key means for monitoring and researching tropospheric NO_2 vertical column concentrations [20–23]. Satellite remote sensing methods offer advantages such as extensive coverage, long time spans, and high spatial and temporal resolutions, which enable efficient and dynamic monitoring of the trends and distribution characteristics of NO_2 atmospheric pollutants. From the 1990s to the present, various sensors have been sequentially used to monitor tropospheric NO_2 vertical column concentrations, including GOME (The Global Ozone Monitoring Experiment, 1996–2003), SCIAMACHY (Scanning Imaging Absorption Spectrometer for Atmospheric Cartography, 2002–2012), OMI (Ozone Monitoring Instrument, 2004 to present), GOME-2 (METOP-A) (2007 to present), GOME-2 (METOP-B) (2013 to present), and TROPOMI (Tropospheric Monitoring Instrument, 2017 to present) [24–27]. Among these, Sentinel-5P, a global atmospheric pollution monitoring satellite launched by the European Space Agency (ESA) in October 2017, carries the Tropospheric Monitoring Instrument (TROPOMI), which represents the latest advancement in satellite atmospheric monitoring. With an imaging swath width of 2600 km, TROPOMI covers the globe daily and can observe trace gas components in the atmosphere, including NO_2, O_3, SO_2, HCHO, CH_4, and CO, which are closely related to human activities. Compared to the above sensors, TROPOMI offers the highest resolution, improved to 3.5 km $\times$ 7 km, with a signal-to-noise ratio increased by one to five times [28], and also enhances observations of aerosols, clouds, etc. [29,30]. Scholars have conducted in-depth validations and applied research on tropospheric NO_2 vertical column concentrations based on the inversion data from these sensors [31–38], with a substantial body of mature research results and reports available on aspects such as NO_2 vertical column density algorithms, inversion techniques, ground validation, and error analysis [39–42]. In China, significant progress has been made in the observation of tropospheric NO_2 vertical column concentrations using satellite remote sensing data in economically developed areas such as the Beijing, Tianjin and Hebei, Yangtze River Delta, and Pearl River Delta regions [42–47]. Simultaneously, some scholars have studied the trends of NO_2 concentrations in China's four major plateau areas [47–50]. However, research on the spatial–temporal variations of tropospheric NO_2 vertical column concentrations in Guizhou Province, with its complex geographical environment and relatively weaker economic development, is relatively scarce.

The spatial–temporal distribution of tropospheric NO_2 column concentrations is comprehensively influenced by human activities, topography, and climate. For instance, Liu et al. [45] analyzed using the OLS model and demonstrated that GDP, population density, and the level of urbanization are the main driving factors for the increase in NO_2 concentrations in China. He et al. [51] found that the characteristics of NO_2 concentration changes in the Yangtze River Delta region are influenced by both human activities such as fossil fuel combustion and vehicle emissions, and natural conditions such as regional topography surface cover, and climate. Zheng et al. [32], in their study of the Guangdong–Hong Kong–Macao Greater Bay Area, discovered that human activities, vegetation conditions, and topographic factors are all significantly correlated with the distribution of tropospheric NO_2 column concentrations. Liu et al. [52] showed that the variation in NO_2 concentrations in the typical plateau city of Kunming is closely related to vehicle exhaust emissions. These studies collectively indicate that the distribution of NO_2 is subject to a complex interplay of human activities, topography, and climate, with varying dominant factors in different regions. For example, Cui et al. [53] and others found that coal consumption is the primary factor contributing to NO_2 pollution in the western provinces of China, while Jiang et al.'s [54] research suggests that the urbanization rate is the main factor affecting NO_2 concentration distribution in the eastern regions of China. The influencing factors of atmospheric environment are complex and regionally variable; therefore, the analysis of factors affecting NO_2 pollution requires in-depth research that considers the geographical, climatic, and social activity characteristics of plateau mountainous areas. Currently, most studies on these areas focus only on the impact of either socio-economic factors or natural factors, with relatively few studies integrating both for comprehensive analysis [55]. The analysis of these influencing factors mostly adopts linear regression methods, such as ordinary least squares and geographically weighted regression [56,57]. Although these methods are simple and practical, they fail to capture the nonlinear relationships of factors affecting the spatial–temporal differentiation of NO_2 column concentrations. In contrast, the Geodetector method, by transforming factors into categorical variables and without the need for linear assumptions, can be used to measure spatial differentiation. It is believed that when an independent variable has a significant impact on a dependent variable, the spatial distribution of the independent and dependent variables shows strong consistency. This method can better explain the degree of influence and nonlinear composite effects of natural and social factors on the spatial–temporal distribution of NO_2 column concentrations [58].

The study utilizes Sentinel-5P satellite inversion data obtained from the GEE platform, combined with spatial statistical analysis models, to investigate the spatial–temporal distribution characteristics of tropospheric NO_2 column concentrations in Guizhou Province. By employing the Geodetector to analyze the influencing factors of NO_2 column concentrations, the research aims to provide important scientific references for improving air quality, formulating, and implementing effective air pollution control policies, and achieving sustainable ecological and environmental development.

2. Data Sources and Methods

2.1. Study Area

Guizhou Province (103°36′~109°35′ E, 24°37′~29°13′ N) is located in the southwestern part of China, situated on the Yunnan-Guizhou Plateau, with a total area of 176,200 km^2. The terrain slopes from west to east, with the central part higher than the northern, eastern, and southern parts. The province's landscape is primarily characterized by plateau mountains, with an average elevation of 1100 m (Figure 1). The average annual temperature ranges from 14 to 16 °C, and the average annual precipitation ranges from 800 to 1700 mm. The climate is mild with abundant rainfall, classified as a subtropical monsoon climate. Guizhou Province serves as an important ecological barrier in the upper reaches of the Yangtze River and the Pearl River. Compared to the serious air pollution problems caused by urbanization and industrialization in the central and eastern regions of China, Guizhou Province generally exhibits a cleaner atmospheric environment with good air quality. However, due to significant regional variations, mountainous terrain, diverse meteorological conditions, and the process of economic development and industrialization, the accumulation of atmospheric pollutants poses challenges to the overall air quality in the region [19].

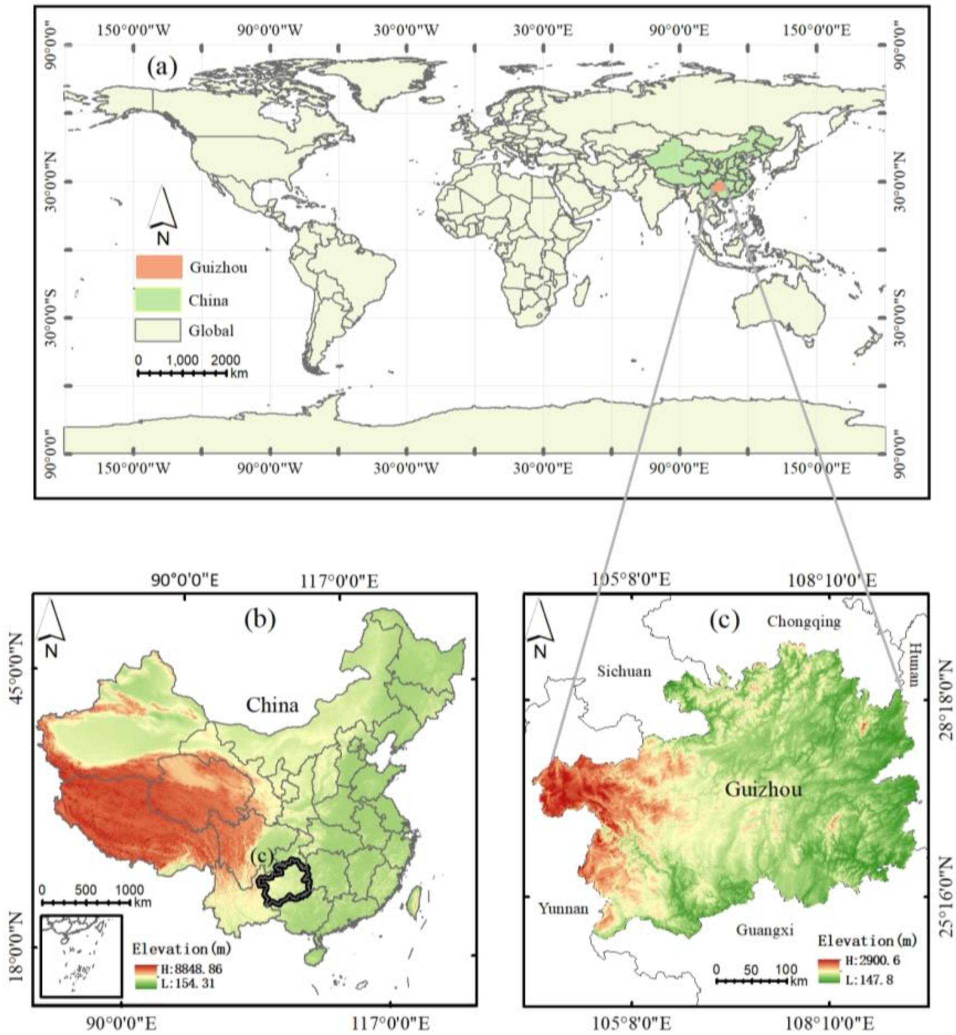

Figure 1. Elevation distribution map of Guizhou Province. (**a**) Global map distribution, (**b**) China elevation distribution map, (**c**) Guizhou elevation distribution map).

2.2. Data Sources

GEE is a remote sensing big data processing platform based on Google Cloud Computing. Its efficient computational power meets the needs for geographical spatial data analysis and interactive computation on a global scale. Utilizing the GEE platform, we obtained the Near Real-Time (NRTI) NO_2 data product derived from Sentinel-5P satellite observations for Guizhou Province from January 2019 to January 2023. Pixels with QA values below 50 were filtered out to ensure the quality of the images, and monthly mean composites were generated. The code can be accessed via the provided link: https://code.earthengine.google.com/ec520da7d969a05779dab20513d53daf (accessed on 1 September 2024). The ground-level NO_2 concentration data for the nine prefecture-level cities in Guizhou Province was sourced from the China Air Quality Monitoring Platform (https://www.aqistudy.cn/ (accessed on 1 September 2024)), which provides continuous monthly average monitoring data from 33 monitoring stations. Meteorological data, including precipitation, temperature, and wind speed, were obtained from ERA5 (the fifth generation of ECMWF atmospheric reanalysis global climate data). The NDVI data were derived from the MOD13A2 16-day composite product, and the DEM data came from the Geospatial Data Cloud's "SRTM Digital Elevation Data", with a resolution of 30 m. Socio-economic data, including population density, regional GDP, and industrial data, were sourced from the Guizhou Statistical Yearbook (2019–2022), selecting data at the city administrative level.

Using ArcGIS 10.2 software, we performed mask analysis of the obtained NO_2 column concentration data according to the administrative boundaries of Guizhou Province, removing anomalous observations below -0.001 mol/m^2 and addressing missing values using spatial interpolation methods. We employed geographic detectors to analyze the influencing factors of NO_2 concentration. To ensure spatial resolution consistency, the DEM, population data, NDVI, and other raster data were resampled to 3.5 km × 3.5 km. The methods and processes used in this study are depicted in Figure 2, and the data utilized are summarized in Table 1.

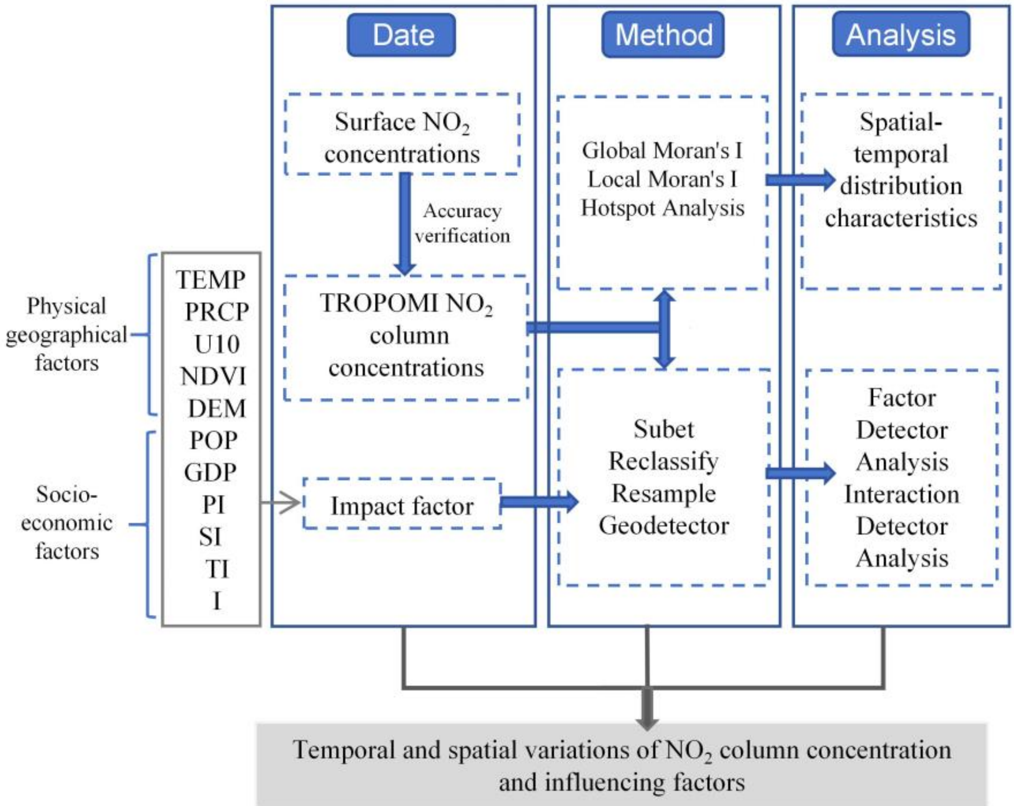

Figure 2. Research method flowchart.

Table 1. Data and sources.

Variable	Indicator	Abbreviation	Source	Unit
NO_2	TROPOMI NO_2 column concentrations	-	Google Earth Engine	mol·m^{-2}
	Surface NO_2 concentrations	-	China National Environmental Monitoring Centre	μg·m^{-3}
Physical geographical factors	Temperature	TEMP	Google Earth Engine	°C
	Precipitation	PRCP		mm
	10 m u-component of wind	U10		-
	Normalized Difference Vegetation Index	NDVI	Google Earth Engine	-
	Digital Elevation Model	DEM	Geospatial Data Cloud	m
Socio-economic factors	Population	POP	Guizhou Province Statistical Yearbook	10,000 persons
	Gross Domestic Product	GDP		CNY 100 million
	Primary Industry	PI		
	Secondary Industry	SI		
	Tertiary Industry	TI		
	Industry	I		

2.3. Methods

2.3.1. Spatial Autocorrelation

Global spatial autocorrelation analysis can be used to examine the spatial association and differentiation of NO_2 column concentrations across the entire study area [59,60]. Specifically, Moran's I index is utilized to describe the spatial association with NO_2 column concentrations throughout the study region. When Moran's I index is greater than 0, it indicates a positive spatial correlation among NO_2 column concentration values, with higher values suggesting stronger spatial clustering. Conversely, smaller values suggest a more dispersed distribution of NO_2 column concentrations, indicating lower spatial clustering. The calculation formula is as follows:

$$I = \frac{n \sum_{i=1}^{n} \sum_{j=1}^{n} w_{ij}(x_i - \bar{X})(x_j - \overline{X})}{\left(\sum_{i=1}^{n} \sum_{j=1}^{n} w_{\mathrm{ij}}\right) \sum_{i=1}^{n} (x_i - \bar{X})} \quad (1)$$

where x_i and x_j represent the tropospheric NO_2 concentration values for the i-th and j-th years, respectively; $w_{i,j}$ denotes the spatial weights matrix, with a value of 1 for adjacent locations and 0 for non-adjacent locations; $\overline{X}$ is the mean NO_2 concentration over multiple years.

2.3.2. Hotspot Analysis

The hotspot analysis is employed to investigate the spatial clustering characteristics of tropospheric NO_2 column concentrations in the study area. This method can reflect high-value and low-value aggregation areas of NO_2 column concentrations at the local spatial level [61,62]. The calculation formula is as follows:

$$G_i^* = \frac{\sum_{j=1}^{n} w_{i,j} x_j - \overline{X} \sum_{j=1}^{n} w_{i,j}}{S \sqrt{\frac{\left[n \sum_{j=1}^{n} w^2{}_{i,j} - \left(\sum_{j=1}^{n} w_{i,j}\right)^2\right]}{n-1}}} \quad (2)$$

where x_j represents the tropospheric NO_2 column concentration value for the j-th year; $w_{i,j}$ denotes the spatial weights matrix, with a value of 1 for adjacent locations and 0 for non-adjacent locations; S represents the standard deviation; $\overline{X}$ is the mean NO_2 column concentration over multiple years. When the value of G_i^* is greater than 0, it indicates that the area is a high-value aggregation area (hot spot); when the value of G_i^* is less than 0, the area is a low-value aggregation area (cold spot).

2.3.3. Geodetector

Geodetector is a statistical method used to analyze and reveal the driving factors of spatial differentiation of geographical phenomena [58]. It includes four detectors: factor detector, interaction detector, risk zone detector, and ecological detector. The explanatory power (q value) is used to measure the extent to which independent variables explain the spatial heterogeneity of dependent variables. Referring to previous research results and data availability [13,15,28,29], a total of 11 influencing factors were selected, including climate factors (annual precipitation, annual temperature, annual wind speed), topographic factors (elevation), socio-economic factors (population density, GDP, value added of the primary industry, value added of the secondary industry, value added of the tertiary industry, industrial output), and other factors (NDVI). These influencing factors were reclassified into nine categories using the natural break point method. The study mainly utilized factor detection and interaction detection for analysis. The factor detector can detect the explanatory power of independent variables (the 11 influencing factors mentioned above) on the spatial differentiation of dependent variables (NO_2 column concentration), with the magnitude measured by the q value. The larger the q value, the stronger the explanatory power. The calculation formulas are as follows:

$$SSW = \sum_{h=1}^{L} N_h \sigma_h^2 \quad (3)$$

$$SST = N\sigma^2 \quad (4)$$

$$q = 1 - \frac{SSW}{SST} = 1 - \frac{\sum_{h=1}^{L} N_h \sigma_h^2}{N\sigma^2} \quad (5)$$

where SSW and SST represent the within sum of squares and total sum of squares, respectively, where $h = 1, 2, \ldots, L$ denotes the stratification or zoning of independent variables. N_h and N represent the number of units in stratum h and the entire area, respectively, while σ_h^2 and σ^2 represent the variance of dependent variable values in stratum h and the entire area, respectively. The range of q values is [0, 1].

The interaction detector can explore the explanatory power and extent of interaction between two factors on the dependent variable or determine whether factors independently affect NO_2 column concentration. The types of interactions are listed in Table 2.

Table 2. Interaction type of two factors.

Classification Basis	Interaction
q(X1∩X2) < Min[q(X1),q(X2)]	Non-linear weak
Min[q(X1),q(X2)] < q(X1∩X2) < Max[q(X1),q(X2)]	Single factor non-linear weak
q(X1∩X2) > Max[q(X1),q(X2)]	Bi-factor enhancement
q(X1∩X2) = q(X1) + q(X2)	Independent
q(X1∩X2) > q(X1) + q(X2)	Non-linear enhancement

3. Results

3.1. Correlation between Sentinel-5P NO_2 Column Concentration and Ground Measured Values

The tropospheric NO_2 column concentration retrieved by the TROPOMI sensor aboard Sentinel-5P has been validated to have a strong correlation with surface NO_2 concentrations. Although there may be an underestimation of NO_2 column concentrations during the retrieval process, the consistency evaluation results between the retrieved data and ground observations reach up to 85% on a global scale, adequately reflecting the variation characteristics of near-surface NO_2 [63]. This study performed a linear fit between the monthly average surface monitoring NO_2 concentrations in Guizhou Province and the monthly average tropospheric NO_2 column concentrations retrieved from Sentinel-5P. The results (Figure 3) show an R^2 value of 0.752, indicating a good linear correlation and consistency, with the concentration distribution trends remaining largely unchanged. Through Pearson correlation analysis, the correlation coefficient was 0.825 ($p = 0.01$), demonstrating a significant positive correlation between the ground-level NO_2 concentrations monitored in Guizhou and the NO_2 column concentrations retrieved from Sentinel-5P. These findings suggest that the tropospheric NO_2 column concentration data retrieved from the Sentinel-5P satellite have high feasibility for addressing the spatial–temporal differentiation characteristics of NO_2 pollution in Guizhou Province, further exploring the potential of using Sentinel-5P atmospheric pollution satellite data in plateau and mountainous regions.

3.2. Spatial–Temporal Distribution Characteristics of Tropospheric NO_2 Column Concentration

3.2.1. Temporal Variations of NO_2 Column Concentration

This study statistically analyzed the changes in the monthly average tropospheric NO_2 column concentrations in Guizhou Province from January 2019 to December 2022 (Figure 4a). The low values of the monthly average NO_2 column concentrations from 2019 to 2022 generally occurred in July and August, during which solar radiation is strong, temperatures are high, and rainfall is abundant, resulting in significant wet deposition that helps reduce NO_2 column concentrations. From July and August to December, the NO_2 column concentrations exhibited an increasing trend, reaching high values from December to January of the following year. This is attributed to relatively weak solar radiation during this period, which reduces the photochemical effects of NO_2 and allows it to remain in the atmosphere for longer periods [64,65]. The maximum monthly average NO_2 column concentration occurred in January 2021, at 4.78×10^{-5} mol/m^2, while the lowest value was recorded in August 2022, at only 1.74×10^{-5} mol/m^2.

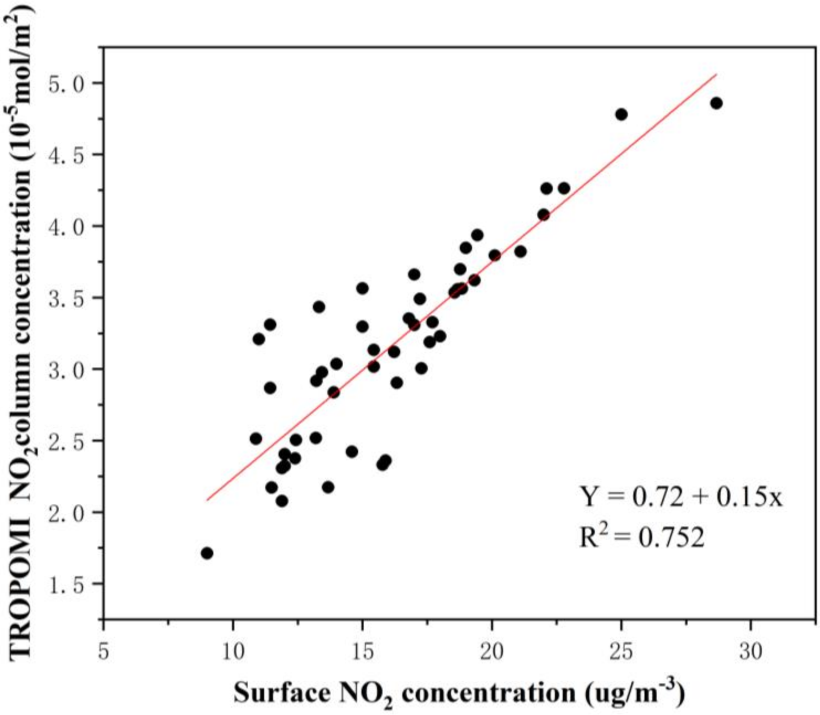

Figure 3. Linear fitting between tropospheric NO_2 column concentration and ground measured values.

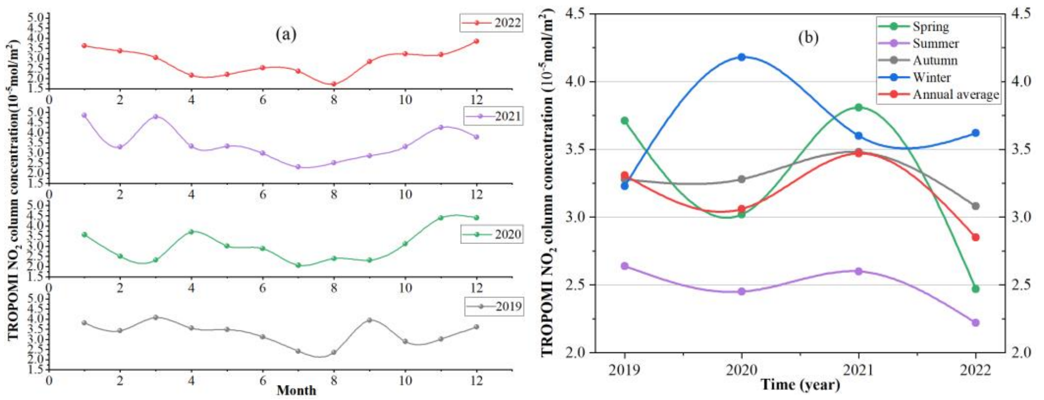

Figure 4. Time variation chart of NO_2 column concentration in Guizhou Province from 2019 to 2022 (note: (**a**) represents the monthly average column concentration variation of NO_2, (**b**) represents the seasonal and annual average column concentration variation trend of NO_2).

The monthly average NO_2 column concentrations for Guizhou Province from 2019 to 2022 were also statistically analyzed by season and year (Figure 4b). Seasonal differences in NO_2 column concentrations were significant, exhibiting a pattern of "highest in winter, lowest in summer, and transitional in spring and autumn". The winter NO_2 column concentration in 2020 reached a maximum of 4.18×10^{-5} mol/m^2, whereas the summer concentration in 2022 was the lowest at only 2.22 × 10^{-5} mol/m^2. By calculating the seasonal average NO_2 column concentrations over the four years, the spring average concentration was 3.25 × 10^{-5} mol/m^2, summer 2.48 × 10^{-5} mol/m^2, autumn 3.28 × 10^{-5} mol/m^2, and winter 3.66 × 10^{-5} mol/m^2. The winter average concentration was 1.48 times that of the summer average concentration, which was the lowest and showed minimal variation, indicating significant seasonal changes.

The annual average NO_2 column concentrations generally displayed a trend of first decreasing, then increasing, and then decreasing again. The highest annual average NO_2 concentration was observed in 2021, reaching 3.47 × 10^{-5} mol/m^2, while the lowest concentration in 2022 was 2.85 × 10^{-5} mol/m^2. The four-year average annual NO_2 column concentration for Guizhou Province was 3.17 × 10^{-5} mol/m^2, indicating that the variation in NO_2 column concentrations over the four years was relatively stable, reflecting good air quality. This stability can be attributed to the "Guizhou Province's Three Year Action Plan for Winning the Blue Sky Defense War" implemented in 2018 [66], which strengthened the management of air pollution in Guizhou Province. Specific measures targeting NO_2 column concentrations were outlined in this action plan, such as enhancing the control of scattered coal pollution sources, promoting new clean energy, and encouraging the use of new energy vehicles, all contributing to the control of NO_2 column concentrations.

3.2.2. Spatial Variation of NO_2 Column Concentration

The annual average column concentration of NO_2 in Guizhou Province from 2019 to 2022 shows an uneven spatial distribution (Figure 5), with a clear pattern of higher concentrations in the west and lower concentrations in the east, as well as higher concentrations in the north and lower concentrations in the south. The northwestern region, including areas east of Bijie, southern Zunyi, Guiyang, Liupanshui, northern Anshun, and northern Qianxinan, has relatively high NO_2 column concentration values, displaying a concentrated and contiguous distribution. Among the high-value distribution areas, Guiyang has the widest spatial distribution range for the annual average NO_2 column concentration. In contrast, the eastern and southern regions, including Qiandongnan, Tongren, and Qiannan, have relatively low NO_2 column concentration values; the atmospheric environment is more stable.

3.3. The Spatial Aggregation and Evolution Characteristics of NO_2 Concentration

This study investigates the annual mean column concentrations of tropospheric NO_2 in Guizhou Province from 2019 to 2022 using spatial autocorrelation methods to examine the spatial aggregation evolution characteristics of NO_2 column concentrations. The x-axis in Figure 6 represents the standardized values of the observed data, calculated by subtracting the mean of the original observations and then dividing by the standard deviation. The y-axis represents the standardized values of the spatial lag of the observed data, which is the weighted average of the neighboring values minus the mean, divided by the standard deviation. The global Moran's I index in the figure passed the significance test (p = 0.01), with values ranging from 0.990 to 0.701, indicating a significant spatial aggregation characteristic of NO_2 column concentrations in the study area, with varying degrees of aggregation. Further analysis of the time series of the global Moran's I index reveals that the index peaked in 2021, suggesting that the spatial aggregation of annual mean tropospheric NO_2 column concentrations was strongest in that year. In contrast, the Moran's I index for 2022 reached its lowest value, indicating a relatively lower degree of spatial aggregation of tropospheric NO_2 column concentrations compared to other years. This result indicates that the spatial aggregation evolution characteristics of tropospheric NO_2 column concentrations in Guizhou Province from 2019 to 2022 are generally consistent with the temporal trends of annual mean NO_2 column concentrations. The scatter points in Figure 6 represent the distribution pattern of the local Moran's I index, which measures the spatial autocorrelation between each individual observation and its neighboring values. The upper part of the scatter plot (high values) shows a clustered pattern, indicating that areas with high concentrations of NO_2 tend to be adjacent to other high-concentration areas.

In contrast, the lower part of the scatter plot from 2020 to 2022 displays a vertical distribution trend, reflecting a weakened clustering effect of low NO_2 column concentrations. Therefore, to analyze the spatial variation of tropospheric NO_2 column concentrations within Guizhou Province, we utilized cold and hot spot analysis and local spatial autocorrelation statistics. The spatial aggregation analysis results indicate that the NO_2 column concentration cold and hot spot areas both exhibit a patchy distribution (Figure 7a1) and pass the 95% significance test. The analysis of local spatial autocorrelation (Figure 7b1) shows that a significant autocorrelation relationship exists for NO_2 column concentrations across most areas in Guizhou, primarily characterized by high–high clusters and low–low clusters. The hotspot areas are consistent with the distribution of high-value aggregation areas, with no significant changes, mainly concentrated in Guiyang, Liupanshui, Bijie, Zunyi, and Anshun. The low-value aggregation areas align with the cold spot areas and exhibit a temporal variation pattern, with a wider distribution range in 2019 and 2021, while the distribution range narrowed in 2020 and 2022, primarily focusing on Tongren, Qiandongnan Prefecture, and southern Qiannan.

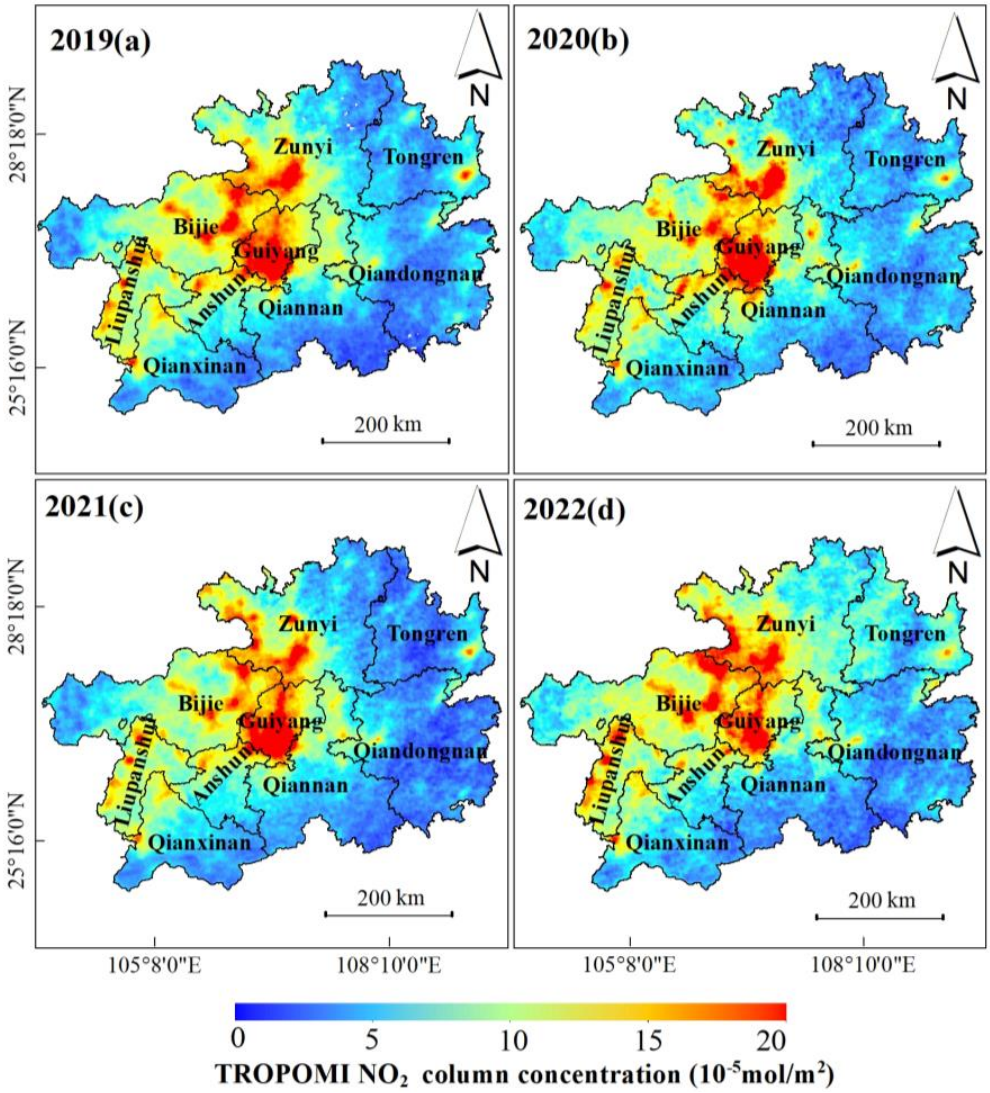

Figure 5. Annual mean spatial distribution of NO_2 column concentration in Guizhou Province from 2019 to 2022.(note: (**a**) Spatial and temporal distribution map of NO_2 column concentration in 2019, (**b**) Spatial and temporal distribution map of NO_2 column concentration in 2020, (**c**) Spatial and temporal distribution map of NO_2 column concentration in 2021, (**d**) Spatial and temporal distribution map of NO_2 column concentration in 2022).

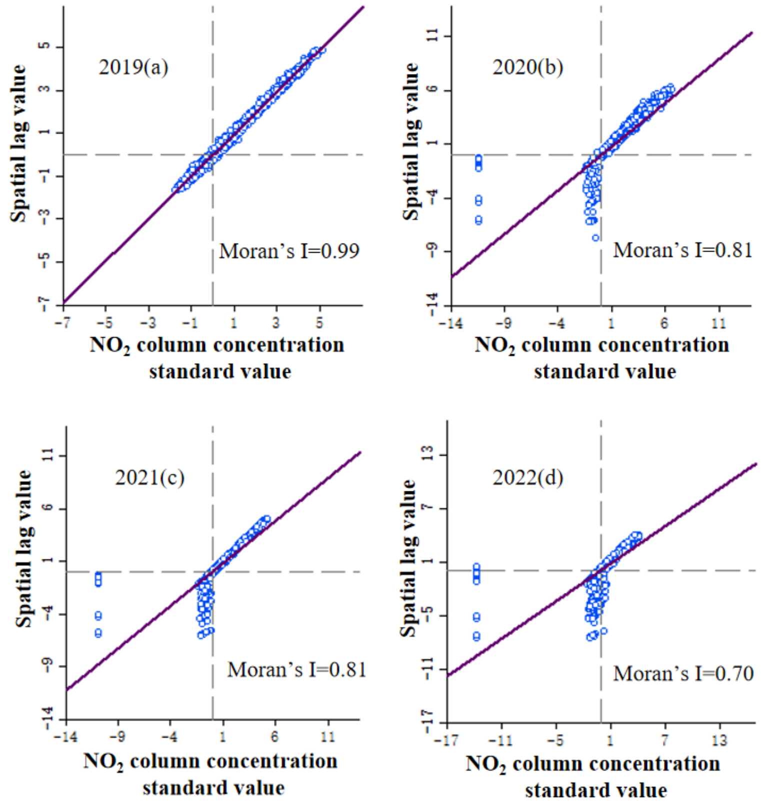

Figure 6. NO_2 column concentration Global Moran's I index map.(note: (**a**) 2019 Global Moran's I index map, (**b**) 2020 Global Moran's I index map, (**c**) 2021 Global Moran's I index map, (**d**) 2022 Global Moran's I index map. The scatter points in the figure represent the observed values, which are the standard NO_2 column concentration values and their spatial lag values for each region. The purple line is a regression line that shows the linear relationship between the standard NO_2 column concentration and its spatial lag value).

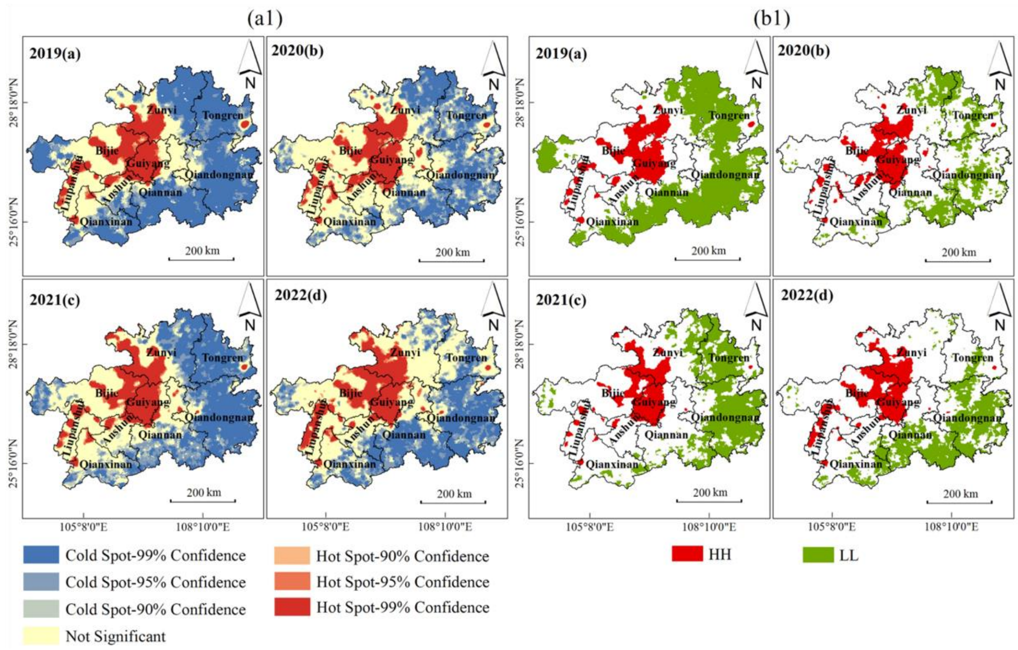

Figure 7. Local spatial aggregation distribution of NO_2 column concentration in Guizhou Province from 2019 to 2022. (note: In the (**a1**) figure, the distributions of NO_2 column concentration hotspots and cold spots are shown for (a) 2019, (b) 2020, (c) 2021, and (d) 2022. In the (**b1**) figure, the Local Moran's index index of NO_2 column concentration is shown for (a) 2019, (b) 2020, (c) 2021, and (d) 2022).

3.4. The Influencing Factors of NO_2 Column Concentration

3.4.1. Factor Detector Analysis

The results from Table 3 indicate that the spatial–temporal distribution of NO_2 column concentration is influenced differently by various factors, with explanatory power ranging from 5% to 46%. Among them, the factors of industry (I), secondary industry (SI), gross domestic product (GDP), and wind speed (U10) have q-values of 30% or above, making them the primary influencing factors of NO_2 column concentration in Guizhou. In addition to the aforementioned factors, tertiary industry (TI), population density (POP), and precipitation (PRCP) are also important influencing factors of NO_2 column concentration variation in Guizhou.

Table 3. Q values of the influencing factors on NO_2 column concentration in Guizhou Province.

Factor Indicators	2019	2020	2021	2022	
	q Value				Average Value
TEMP	0.21 *	0.13 *	0.25 *	0.25 *	0.21
PRCP	0.24 *	0.29 *	0.28 *	0.25 *	0.27
U10	0.29 *	0.35 *	0.31 *	0.46 *	0.35
NDVI	0.09 *	0.05 *	0.09 *	0.09 *	0.08
DEM	0.18 *	0.19 *	0.19 *	0.12 *	0.17
POP	0.32 *	0.28 *	0.30 *	0.26 *	0.29
GDP	0.36 *	0.31 *	0.38 *	0.39 *	0.36
PI	0.14 *	0.15 *	0.15 *	0.23 *	0.17
SI	0.42 *	0.37 *	0.46 *	0.35 *	0.40
TI	0.33 *	0.32 *	0.32 *	0.29 *	0.31
I	0.42 *	0.40 *	0.46 *	0.45 *	0.43

Note: (*) indicates that the influencing factor is significant at the 1% level.

By comparing the various influencing factors (Table 4), it can be observed that the q-values of industry (I) and secondary industry (SI) remain stable, indicating that socio-economic activities have a greater impact on NO_2 column concentration, as economic development consumes energy and leads to increased waste, thus causing air pollution. The significant variations in the q-values of wind speed (U10) and precipitation (PRCP) are attributed to the complex terrain and diverse ecological environments in Guizhou. Different climatic, hydrological, and thermal factors among the various ecological environments result in differences in NO_2 decomposition, residence time, etc. [67]. Additionally, wind speed directly affects the diffusion rate and direction of atmospheric pollutants [68]. Due to the inhibitory effects of heavy rainfall and moist environments on the growth of NO_2 concentration, atmospheric pollutants are more likely to diffuse and dilute in humid environments, making it difficult for them to accumulate for extended periods [51]. Thus, wind speed and precipitation emerge as important climatic factors influencing the variation of NO_2 column concentration. Overall, this suggests that human activities exert a significantly stronger influence on NO_2 column concentration in Guizhou Province, followed by climatic factors.

Table 4. Ranking table of Q Values of the main influencing factors from 2019 to 2022.

Year	q Value Sorting
2019	q(I) = q(SI) > q(GDP) > q(TI) > q(POP) > q(U10) > q(PRCP)
2020	q(I) > q(SI) > q(U10) > q(TI) > q(TI) > q(GDP) > q(PRCP) > q(POP)
2021	q(I) = q(SI) > (GDP) > q(TI) > q(U10) > q(POP) > q(PRCP)
2022	q(U10) > q(I) > q(GDP) > q(SI) > q(TI) > q(POP) > q(PRCP)

3.4.2. Interactive Detector Analysis

The interaction detector can be used to analyze the mutual comprehensive effects between human activity factors and natural factors on NO_2 column concentrations, determining whether they enhance, weaken, or act independently. The study results indicate (Figure 8) that the interaction between any two factors enhances the explanatory power of individual factors on NO_2 column concentrations. There are two types of relationships under the superposition of any two factors: dual-factor enhancement and nonlinear enhancement. Among these relationships, dual-factor enhancement is the majority, implying that the superposition of factors has a strong driving effect on the changes in NO_2 concentrations. By comparing the factor interaction detection results from 2019 to 2022, the q values of the interactions among factors range between 5 and 69%, with the maximum value occurring in 2019, at a q value of 0.69. The minimum value was in 2020, with a q value of 0.05. Moreover, each year's maximum q value is the result of the interaction between socio-economic factors and other factors, indicating that the interaction between socio-economic factors and other factors is stronger than the interactions among other factors. This suggests that socio-economic development has a significant impact on NO_2 concentrations. Overall, the influence of various factors on the changes in NO_2 concentrations is not independent but exhibits significant interplay. Furthermore, the impact of multiple factors' interactions on NO_2 concentration changes is not a simple superposition process but rather a dual-factor or nonlinear enhancement. As a researcher, this translation adheres to the grammatical and syntactical standards appropriate for English academic papers.

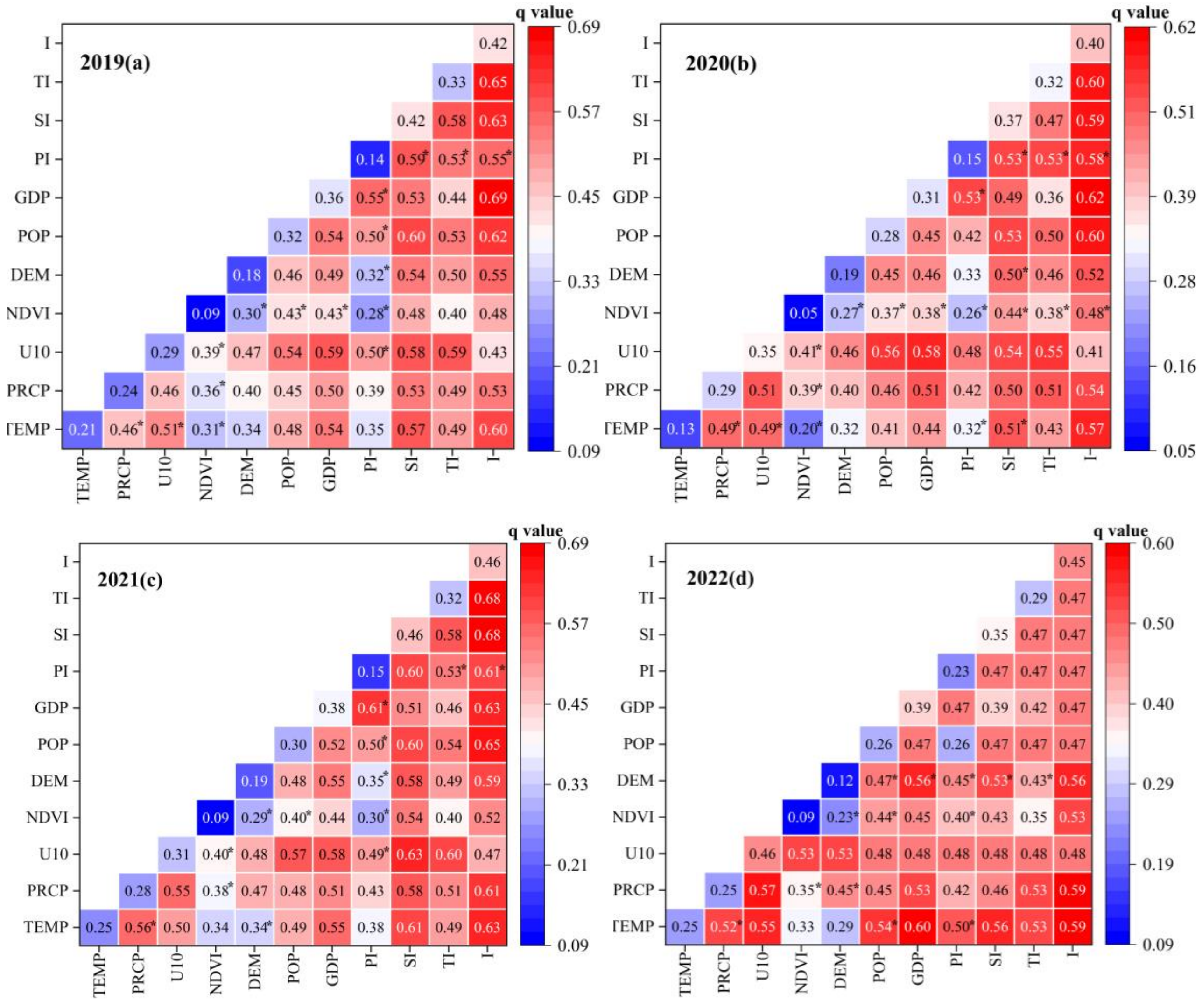

Figure 8. Interaction of factors influencing NO_2 column concentration. ((*) indicates that the interaction between two factors is non-linear enhancement, while the rest is linear enhancement).

4. Discussion

4.1. Spatial–Temporal Distribution Characteristics of NO_2 Column in Highland

This section explores the spatial–temporal distribution characteristics of NO_2 column concentration in the high-altitude mountainous region of Guizhou Province. Spatially, the overall distribution of NO_2 column concentration aligns with economic development patterns. Data from the statistical yearbook from 2019 to 2022 reveal that the western and northern regions of Guizhou account for 70% of the province's GDP, 76.33% of its industrial output, 73% of its resident population density, and 89% of its civilian vehicle ownership. This indicates that these areas have stronger economies, higher industrial proportions, greater population densities, and more vehicles, leading to increased NO_2 emissions. High-value and hot spot areas are primarily found in regions with higher population densities and socio-economic activities. For instance, Guiyang, the provincial capital, has the highest GDP and population density, accounting for 19% of the province's industrial output, resulting in significant NO_2 emissions. In contrast, low-value and cold spot areas, like Qiandongnan Prefecture, show slower economic development and a low population density of only 123.485 people per square kilometer, contributing just 3.03% to the province's industrial output. Therefore, for areas with high NO_2 concentration, a comprehensive photochemical monitoring network can be established, promoting regional joint prevention and control measures, information sharing, and coordinated governance to mitigate NO_2 pollution.

Seasonally, NO_2 column concentrations are highest in winter and lowest in summer. Previous research indicates that seasonal variations in NO_2 concentrations in Guizhou are primarily due to meteorological differences [69–71]. The province experiences substantial rainfall in summer, which disperses, dilutes, and absorbs NO_2 pollutants. Additionally, increased atmospheric convection during summer and stronger solar radiation promote reactions between NO_2 and OH radicals, resulting in HNO_3 formation and aiding NO_2 photolysis and O_2 reactions to produce O_3, which facilitates the removal of NO_2 through wet and dry deposition. In winter, shorter daylight hours and weaker solar radiation contribute to stable temperature inversions, hindering vertical air movement and trapping NO_2 pollutants. Coupled with lower precipitation and increased fossil fuel usage for heating, winter NO_2 emissions rise, leading to the highest concentrations during this season.

Overall, from 2019 to 2022, the average annual NO_2 column concentration in Guizhou remained low and stable. Compared to air pollution issues caused by urbanization and industrialization in central and eastern China, Guizhou's relatively low population density and limited industrial development contribute to reduced traffic and industrial activities, thereby lowering NO_2 emissions. Furthermore, since 2013, Guizhou has implemented a series of environmental protection policies and measures [72–74], resulting in a relatively clean atmospheric environment and good air quality, consistent with findings from other scholars [75–77].

4.2. Factors Influencing NO_2 Column Concentration

Research indicates that human activities are the primary factor influencing the tropospheric NO_2 column concentrations in Guizhou Province. This finding aligns with the spatial aggregation results of NO_2 concentrations, showing that better socio-economic development and higher population density correlate with increased NO_2 levels. Notably, among economic factors, industrial activities dominate, accounting for 46% of the variance in NO_2 concentrations according to geographical detectors. Industrial production is a significant source of tropospheric NO_2 emissions due to high energy consumption from processes like coal mining, thermal power generation, and chemical processing, leading to increased NO_2 levels and substantial impacts on the atmospheric environment. Effective measures to control air pollution include developing clean energy and efficient power industries, addressing scattered coal burning, reducing coal consumption, and adjusting industrial structures at the municipal level. Additionally, wind speed and rainfall are two critical meteorological factors affecting the temporal and spatial variations of NO_2

concentrations. Guizhou's subtropical humid climate had annual rainfall ranging from 1014.2 to 1448.3 mm between 2019 and 2022, which helped to wash away and suppress NO_2, resulting in distinct monthly and seasonal concentration variations. The average summer wind speed in Guizhou ranges from 0.9 to 3.1 m/s, facilitating the rapid dispersion of NO_2 emissions and reducing local accumulation. During summer, prevailing southwest winds lead to lower NO_2 concentrations in upwind areas, while northeast winds in winter can transport higher NO_2 levels from the central region into Guizhou.

Moreover, the factors influencing NO_2 concentrations in Guizhou Province vary across different administrative units. Although industrial factors are the most significant statewide, factors affecting NO_2 levels in cities may differ due to geographic, meteorological, and population density variations. For instance, although Zunyi City had the highest average industrial output from 2019 to 2022, its NO_2 concentration ranked fifth among nine cities. This discrepancy arises from its emissions primarily originating from thermal power and cement industries [78]. Zunyi's low latitude and monsoon influences facilitate NO_2 emissions and dispersion, while proactive pollution prevention measures, including a 2017 "air pollution prevention plan" [79] and the "Blue Sky Protection Campaign" [80] have improved air quality, raising the city's air quality rate to 98.1% in 2019 and maintaining lower NO_2 levels. In contrast, NO_2 concentrations in other cities may be influenced by varying factors such as industrial structure, atmospheric stability, rainfall, emission control measures, and geographical locations. These differences can lead to varying influences and mechanisms between overall and localized conditions. Therefore, future research should further analyze the characteristics of different regions to develop more targeted and refined NO_2 pollution control measures.

4.3. Limitations and Prospects

This study utilizes the GEE cloud platform to process and rapidly obtain NO_2 column concentration data for Guizhou from 2019 to 2022. These data can objectively reflect the spatial evolution trend of NO_2 column concentrations in Guizhou and provide references for air pollution control research. However, since the Sentinel-5P data span from January 2019 to December 2023, further analysis is needed to understand the long-term spatial–temporal variations in tropospheric NO_2 concentrations. Although the study has comprehensively selected several influencing factors such as climate, human activities, and topography, the extent of their explanation varies across different administrative units, which is complex. Future research will consider integrating multi-source data, including OMI satellite data, GEMS satellite data, and ground-based NO_2 monitoring data, to improve the accuracy of tropospheric NO_2 column concentration studies. Additionally, it will take into account the variations in driving factors affecting NO_2 column concentrations at both global and local levels, facilitating a deeper exploration of the changing patterns of NO_2 concentrations.

5. Conclusions

The paper utilized Sentinel-5P satellite remote sensing data to investigate the spatial–temporal variations of NO_2 column concentration in Guizhou Province. Employing spatial statistical methods and geographic detectors, the study systematically analyzed the spatial–temporal patterns and influencing factors of NO_2 column concentration. The conclusions are as follows:

(1) Based on Sentinel-5P satellite remote sensing data, the monthly average NO_2 column concentration was linearly fitted with the monthly average NO_2 concentration from ground monitoring, R^2 = 0.752. The Pearson correlation coefficient was calculated to be 0.825 (p = 0.01), indicating a positive correlation. This suggests that utilizing Sentinel-5P satellite data to study NO_2 column concentrations in the mountainous regions of Guizhou Province is highly feasible.

(2) The NO_2 column concentration in Guizhou Province exhibits a seasonal variation characteristic of "higher in winter, lower in summer, and transitional in spring and autumn". In terms of annual variation, the annual average concentration was highest

in 2021 at 3.47×10^{-5} mol/m^2 and lowest in 2022 at 2.85×10^{-5} mol/m^2. There is an uneven spatial distribution, presenting a pattern of "higher in the west, lower in the east; higher in the north, lower in the south", with significant spatial clustering characteristics. The distribution patterns of cold and hot spots are consistent with those of high- and low-value aggregation areas.

(3) Geodetector analysis reveals that socio-economic factors exert the greatest influence on NO_2 column concentration variations in Guizhou. Industrial factors notably affect NO_2 concentrations, while wind speed and rainfall are also significant climate-related factors. Interactions between any two factors enhance either linearly or non-linearly, with socio-economic factors showing stronger interactions compared to other factors, indicating that economic development has the most significant impact on NO_2 column concentrations.

Author Contributions: Methodology, F.D.; software, F.D. and D.H.; formal analysis, F.D. and X.D.; data curation, S.D.; writing—original draft preparation, F.D.; writing—review and editing, F.D. and Z.Z.; funding acquisition, Z.Z. All authors have read and agreed to the published version of the manuscript.

Funding: This research was funded by the Regional Program of the National Natural Science Foundation of China (Grant No:41661088); the "Hundred" Level Talents of Guizhou Province's High level Innovative Talent Training Program (Grant No:Guizhou Science and Technology Cooperation Platform Talents (2016) 5674).

Institutional Review Board Statement: Not applicable.

Informed Consent Statement: Not applicable.

Data Availability Statement: Sentinel-5P NO_2 data, "MOD13A2 16 d" data, and ERA5 Land were obtained from the Google Earth Engine platform: https://earthengine.google.com (accessed on 1 January 2024); SRTM Digital Elevation Data comes from the Geospatial Data Cloud: https://www.gscloud.cn/ (accessed on 1 January 2024); The NO_2 concentration monitored on the ground was acquired from the China Environmental Monitoring Center: https://www.aqistudy.cn/ (accessed on 1 January 2024). Other influencing factor data Obtain yearbooks from Guizhou Provincial and County Statistics Bureaus from 2019 to 2022.

Conflicts of Interest: The authors declare no conflicts of interest.

References

1. Pope, C.A.; Dockery, D.W. Health Effects of Fine Particulate Air Pollution: Lines that Connect. *J. Air Waste Manag. Assoc.* **2012**, *56*, 709–742. [CrossRef] [PubMed]
2. Lelieveld, J.; Evans, J.S.; Fnais, M.; Giannadaki, D.; Pozzer, A. The contribution of outdoor air pollution sources to premature mortality on a global scale. *Nature* **2015**, *525*, 367–371. [CrossRef] [PubMed]
3. Li, H.; Zhang, Q.; Zheng, B.; Chen, C.; Wu, N.; Guo, H.; Zhang, Y.; Zheng, Y.; Li, X.; He, K. Nitrate-driven urban haze pollution during summertime over the North China Plain. *Atmos. Chem. Phys.* **2018**, *18*, 5293–5306. [CrossRef]
4. Stohl, A.; Aamaas, B.; Amann, M.; Baker, L.H.; Bellouin, N.; Berntsen, T.K.; Boucher, O.; Cherian, R.; Collins, W.; Daskalakis, N. Evaluating the climate and air quality impacts of short-lived pollutants. *Atmos. Chem. Phys.* **2015**, *15*, 10529–10566. [CrossRef]
5. Crutzen, P.J. The role of NO and NO_2 in the chemistry of the troposphere and stratosphere. *Annu. Rev. Earth Planet. Sci.* **1979**, *7*, 443–472. [CrossRef]
6. Lin, J.T.; McElroy, M.B. Detection from space of a reduction in anthropogenic emissions of nitrogen oxides during the Chinese economic downturn. *Atmos. Chem. Phys.* **2011**, *11*, 8171–8188. [CrossRef]
7. Richter, A.; Burrows, J.P.; Nüß, H.; Granier, C.; Niemeier, U. Increase in tropospheric nitrogen dioxide over China observed from space. *Nature* **2005**, *437*, 129–132. [CrossRef]
8. Tian, H.; Xu, R.; Canadell, J.G.; Thompson, R.L.; Winiwarter, W.; Suntharalingam, P.; Davidson, E.A.; Ciais, P.; Jackson, R.B.; Janssens-Maenhout, G. A comprehensive quantification of global nitrous oxide sources and sinks. *Nature* **2020**, *586*, 248–256. [CrossRef]
9. Zheng, B.; Tong, D.; Li, M.; Liu, F.; Hong, C.; Geng, G.; Li, H.; Li, X.; Peng, L.; Qi, J. Trends in China's anthropogenic emissions since 2010 as the consequence of clean air actions. *Atmos. Chem. Phys.* **2018**, *18*, 14095–14111. [CrossRef]
10. Metz, B.; Davidson, O.R.; Bosch, P.R.; Dave, R.; Meyer, L.A. *Contribution of Working Group III to the Fourth Assessment Report of the Intergovernmental Panel on Climate Change*; Cambridge University Press: Cambridge, UK, 2007.

11. Diao, B.; Ding, L.; Su, P.; Cheng, J. The spatial-temporal characteristics and influential factors of NOx emissions in China: A spatial econometric analysis. *Int. J. Environ. Res. Public Health* **2018**, *15*, 1405. [CrossRef]
12. Jia, L.; Ge, M.; Xu, Y.; Du, L.; Zhuang, G.; Wang, D. Progress in Atmospheric Ozone Chemistry. *Prog. Chem.* **2006**, *18*, 1565.
13. Wang, G.; LV, D.; Yang, P. The impact of human activities on the atmospheric ozone layer. *Prog. Earth Sci.* **2009**, *24*, 331.
14. Van Der A, R.; Peters, D.; Eskes, H.; Boersma, K.; Van Roozendael, M.; De Smedt, I.; Kelder, H. Detection of the trend and seasonal variation in tropospheric NO_2 over China. *J. Geophys. Res. Atmos.* **2006**, *111*, D12. [CrossRef]
15. Gu, X.; Li, G.Y.; Chen, Y.; Liao, Y. Research on spatiotemporal differences in pollution gas concentration in Guizhou Province based on OMI and ground monitoring. *J. Atmos. Environ. Opt.* **2024**, *19*, 85–97.
16. Ministry of Ecology and Environment of the People's Republic of China. National Urban Air Quality Report. Available online: https://www.mee.gov.cn/hjzl/dqhj/cskqzlzkyb/ (accessed on 10 October 2024).
17. Ecological Environment Department of Guizhou Province. Guizhou Province Ecological Environment Status Bulletin. Available online: https://sthj.guizhou.gov.cn/zwgk/hjsj/hjzkgb/202305/t20230531_79980089.html (accessed on 10 October 2024).
18. The Central People's Government of the People's Republic of China. The Central Committee of the Communist Party of China on Formulating the 14th Five Year Plan for National Economic and Social Development and the Long Range Objectives for 2035. Available online: https://www.gov.cn/zhengce/2020-11/03/content_5556991.htm (accessed on 10 October 2024).
19. Yang, Y.; Liu, H.; Xu, P.; Feng, P.; Wang, Y. Progress in Air Pollution Prevention and Control in Guizhou Province, Existing Challenges and Suggestions for Countermeasures. *Environ. Prot. Technol.* **2022**, *28*, 1–7+40.
20. David, L.M.; Nair, P.R. Tropospheric column O_3 and NO_2 over the Indian region observed by Ozone Monitoring Instrument (OMI): Seasonal changes and long-term trends. *Atmos. Environ.* **2013**, *65*, 25–39. [CrossRef]
21. Kim, D.-R.; Lee, J.-B.; Song, C.K.; Kim, S.-Y.; Ma, Y.-l.; Lee, K.-M.; Cha, J.-S.; Lee, S.-D. Temporal and spatial distribution of tropospheric NO_2 over Northeast Asia using OMI data during the years 2005–2010. *Atmos. Pollut. Res.* **2015**, *6*, 768–776. [CrossRef]
22. Krotkov, N.A.; McLinden, C.A.; Li, C.; Lamsal, L.N.; Celarier, E.A.; Marchenko, S.V.; Swartz, W.H.; Bucsela, E.J.; Joiner, J.; Duncan, B.N. Aura OMI observations of regional S_2 and NO_2 pollution changes from 2005 to 2015. *Atmos. Chem. Phys.* **2016**, *16*, 4605–4629. [CrossRef]
23. Lu, Z.; Streets, D.G.; De Foy, B.; Krotkov, N.A. Ozone Monitoring Instrument observations of interannual increases in S_2 emissions from Indian coal-fired power plants during 2005–2012. *Environ. Sci. Technol.* **2013**, *47*, 13993–14000. [CrossRef]
24. Bucsela, E.; Celarier, E.; Wenig, M.; Gleason, J.; Veefkind, J.; Boersma, K.; Brinksma, E. Algorithm for NO_2 vertical column retrieval from the Ozone Monitoring Instrument. *IEEE T. Geosci. Remote Sens.* **2006**, *44*, 1245–1258. [CrossRef]
25. Li, L.; Shi, R.; Liu, P.; Zhang, J. Long-term NO_2 monitoring by satellite in the Pearl River Delta. *Remote Sens. Model. Ecosyst. Sustain. X* **2013**, *8869*, 211–219.
26. Bauwens, M.; Compernolle, S.; Stavrakou, T.; Müller, J.F.; Van Gent, J.; Eskes, H.; Levelt, P.F.; Van Der A, R.; Veefkind, J.; Vlietinck, J. Impact of coronavirus outbreak on NO_2 pollution assessed using TROPOMI and OMI observations. *Geophys. Res. Lett.* **2020**, *47*, e2020GL087978. [CrossRef] [PubMed]
27. Burrows, J.P.; Weber, M.; Buchwitz, M.; Rozanov, V.; Ladstätter-Weißenmayer, A.; Richter, A.; DeBeek, R.; Hoogen, R.; Bramstedt, K.; Eichmann, K.-U. The global ozone monitoring experiment (GOME): Mission concept and first scientific results. *J. Atmos. Sci.* **1999**, *56*, 151–175. [CrossRef]
28. Eisinger, M.; Burrows, J.P. Tropospheric sulfur dioxide observed by the ERS-2 GOME instrument. *Geophys. Res. Lett.* **1998**, *25*, 4177–4180. [CrossRef]
29. Zhao, X.; Griffin, D.; Fioletov, V.; McLinden, C.; Cede, A.; Tiefengraber, M.; Müller, M.; Bognar, K.; Strong, K.; Boersma, F. Assessment of the quality of TROPOMI high-spatial-resolution NO_2 data products in the Greater Toronto Area. *Atmos. Meas. Tech.* **2020**, *13*, 2131–2159. [CrossRef]
30. Uno, I.; He, Y.; Ohara, T.; Yamaji, K.; Kurokawa, J.-I.; Katayama, M.; Wang, Z.; Noguchi, K.; Hayashida, S.; Richter, A. Systematic analysis of interannual and seasonal variations of model-simulated tropospheric NO_2 in Asia and comparison with GOME-satellite data. *Atmos. Chem. Phys.* **2007**, *7*, 1671–1681. [CrossRef]
31. Zhang, Q.; Streets, D.G.; He, K.; Wang, Y.; Richter, A.; Burrows, J.P.; Uno, I.; Jang, C.J.; Chen, D.; Yao, Z. NOx emission trends for China, 1995–2004: The view from the ground and the view from space. *J. Geophys. Res. Atmos.* **2007**, *112*, D22. [CrossRef]
32. Zheng, Z.; Wu, Z.; Chen, Y.; Yang, Z. Analysis of spatiotemporal changes of NO_2 pollutants in the Guangdong Hong Kong Macao Greater Bay Area based on Sentinel-5P. *Chin. Environ. Sci.* **2021**, *41*, 63–72.
33. Vîrghileanu, M.; Săvulescu, I.; Mihai, B.-A.; Nistor, C.; Dobre, R. Nitrogen Dioxide ($_2$) Pollution monitoring with Sentinel-5P satellite imagery over Europe during the coronavirus pandemic outbreak. *Remote Sens.* **2020**, *12*, 3575. [CrossRef]
34. Chen, R.; Yin, P.; Meng, X.; Wang, L.; Liu, C.; Niu, Y.; Lin, Z.; Liu, Y.; Liu, J.; Qi, J. Associations between ambient nitrogen dioxide and daily cause-specific mortality: Evidence from 272 Chinese cities. *Epidemiology* **2018**, *29*, 482–489. [CrossRef]
35. Shah, V.; Jacob, D.J.; Li, K.; Silvern, R.F.; Zhai, S.; Liu, M.; Lin, J.; Zhang, Q. Effect of changing NOx lifetime on the seasonality and long-term trends of satellite-observed tropospheric NO_2 columns over China. *Atmos. Chem. Phys.* **2020**, *20*, 1483–1495. [CrossRef]
36. Wei, J.; Liu, S.; Li, Z.; Liu, C.; Qin, K.; Liu, X.; Pinker, R.T.; Dickerson, R.R.; Lin, J.; Boersma, K. Ground-level NO_2 surveillance from space across China for high resolution using interpretable spatiotemporally weighted artificial intelligence. *Environ. Sci. Technol.* **2022**, *56*, 9988–9998. [CrossRef]
37. Chen, D.; Zhou, B.; Beirle, S.; Chen, L.; Wagner, T. Tropospheric NO_2 column densities deduced from zenith-sky DOAS measurements in Shanghai, China, and their application to satellite validation. *Atmos. Chem. Phys.* **2009**, *9*, 3641–3662. [CrossRef]

38. Qin, K.; Rao, L.; Xu, J.; Bai, Y.; Zou, J.; Hao, N.; Li, S.; Yu, C. Estimating ground level NO_2 concentrations over Central-Eastern China using a satellite-based geographically and temporally weighted regression model. *Remote Sens.* **2017**, *9*, 950. [CrossRef]
39. Schneider, P.; Hamer, P.; Kylling, A.; Shetty, S.; Stebel, K. Spatiotemporal Patterns in Data Availability of the Sentinel-5P NO_2 Product over Urban Areas in Norway. *Remote Sens.* **2021**, *13*, 2095. [CrossRef]
40. Fang, K.; Wang, T.; He, J.; Shen, Y. Spatiotemporal variation and driving factors of NO_2 concentration in the Belt and Road region. *Acta Ecol. Sin.* **2020**, *40*, 4241–4251.
41. Guan, Q.D.; Zuo, X.Q.; Li, S.H.; Zhang, H.; Wang, H. Analysis of spatiotemporal variation characteristics and driving factors of atmospheric NO_2 concentration in the Yangtze River Delta urban agglomeration based on OMI data. *J. Guizhou Univ. (Nat. Sci. Ed.)* **2021**, *38*, 115–124.
42. Liu, X.; Zheng, T.; Wan, Q.; Tan, H.; Deng, X.; Li, F.; Deng, T. The spatiotemporal distribution characteristics and human activity impact analysis of NO_2 in the Pearl River Delta urban agglomeration using OMI remote sensing. *J. Trop. Meteorol.* **2015**, *31*, 193–201.
43. Wang, C.; Wang, T.; Wang, P.; Wang, W. Assessment of the performance of TROPOMI NO_2 and SO_2 data products in the North China Plain: Comparison, correction and application. *Remote Sens.* **2022**, *14*, 214. [CrossRef]
44. Müller, I.; Erbertseder, T.; Taubenböck, H. Tropospheric $_2$: Explorative analyses of spatial variability and impact factors. *Remote Sens. Environ.* **2022**, *270*, 112839. [CrossRef]
45. Liu, Y.; Jie, Y.; Guo, Z. Remote sensing monitoring of NO_2 concentration in China based on Sentinel-5P satellite. *Chin. Environ. Sci.* **2022**, *42*, 4983–4990.
46. Isazade, V.; Qasimi, A.B.; Isazade, E. Environmental dust effect phenomenon on the sustainability of urban areas using remote sensing data in GEE. *Saf. Extrem. Environ.* **2022**, *5*, 59–67. [CrossRef]
47. Gao, M.; Zhu, B.; Shi, S.; Jiang, Y.; Fang, K.; Zhao, H.; Wan, H.; Liu, H. Analysis of ozone characteristics and influencing factors in typical cities on the Loess Plateau. *J. Environ. Sci.* **2023**, *43*, 1–13.
48. Zheng, C.; Zhao, C.; Li, Y.; Wu, X.; Zhang, K.; Gao, J.; Qiao, Q.; Ren, Y.; Zhang, X.; Chai, F. Spatial and temporal distribution of NO_2 and S_2 in Inner Mongolia urban agglomeration obtained from satellite remote sensing and ground observations. *Atmos. Environ.* **2018**, *188*, 50–59. [CrossRef]
49. Cheng, S.; Pu, G.; Ma, J.; Hong, H.; Du, J.; Yudron, T.; Wagner, T. Retrieval of Tropospheric NO_2 Vertical Column Densities from Ground-Based MAX-DOAS Measurements in Lhasa, a City on the Tibetan Plateau. *Remote Sens.* **2023**, *15*, 4689. [CrossRef]
50. Liu, Y.; Xiang, F.; Han, X.; Shi, Z.; Wang, C.; Huang, Y.; Shi, J. Pollution characteristics and source analysis of atmospheric VOCs in the central urban area of Kunming in summer and autumn. *J. Yunnan Univ. (Nat. Sci. Ed.)* **2018**, *40*, 104–112.
51. He, Y.; Sheng, M.; Lei, L.; Guo, K.; He, Z.; Cai, J.; Fang, H.; Zhang, X.; Liu, Y.; Zhang, Y. Analysis of spatiotemporal variations and driving factors of atmospheric NO_2 and C_2 concentrations in the Yangtze River Delta region. *Chin. Environ. Sci.* **2022**, *42*, 3544–3553.
52. Yu, L.; He, W.; Li, N.; Lu, J.; Xie, S.; Huang, L.; Fang, Z.; Chao, H.; Zhao, X.; Zhang, M. Analysis of spatiotemporal variation patterns and influencing factors of NO_2 in Guangxi. *Environ. Sci. Technol.* **2021**, *44*, 10036504.
53. Cui, Y.; Jiang, L.; Zhang, W.; Feng, X.; Huang, B. Research on the spatiotemporal distribution and influencing factors of anthropogenic NO_2 pollution in western China. *J. Environ. Sci.* **2019**, *39*, 10.
54. Jiang, J.; Hou, L.; Wang, X.; Wang, L.; Wu, G.; Zhao, W. Distribution characteristics of NO_2 pollution near the ground in China and analysis of its socio-economic influencing factors. *J. Ecol. Environ.* **2019**, *28*, 1632–1641.
55. Kai, F.; Tingting, W.; Jianjian, H.; Yang, S. Temporal and spatial variation characteristics and driving factors of NO_2 concentration along the "the Belt and Road". *J. Ecol. Environ.* **2020**, *40*, 4241–4251.
56. Liu, H.; Fang, C.; Huang, J.; Zhu, X.; Zhou, Y.; Wang, Z.; Zhang, J. Analysis of spatiotemporal characteristics and influencing factors of air pollution in the Beijing Tianjin Hebei urban agglomeration. *Geogr. J.* **2018**, *73*, 177–191.
57. Rui, L.; Zhenzhen, W.; Lulu, C.; Hongbo, F.; Liwu, Z.; Lingdong, K.; Weidong, C.; Jianmin, C. Air pollution characteristics in China during 2015–2016: Spatiotemporal variations and key meteorological factors. *Sci. Total Environ.* **2018**, *648*, 902–915.
58. Wang, J.; Xu, C. Geodetectors: Principles and Prospects. *J. Geogr.* **2017**, *72*, 19.
59. Sokal, R.R.; Oden, N.L. Spatial autocorrelation in biology: 1. *Methodology* **1978**, *10*, 199–228.
60. Yu, R.; Liu, M.; Li, L.; Song, J.; Sun, R.; Zhang, G.; Xu, L.; Mu, R. The spatiotemporal variation and influencing factors of atmospheric ozone column concentration in the Yangtze River Delta region over the past 15 years. *J. Environ. Sci.* **2021**, *41*, 770–784.
61. Zhang, J.J. The Reality and Feasibility of Shanghai Hong Kong Cooperation in the Development of the Russian Far East. *Sib. Stud.* **2017**, *44*, 25–27.
62. Zhang, W.; Zhang, X.; Liu, L.; Zhao, L.; Lu, X. Temporal and Spatial Variation of Atmospheric NO_2 Concentration in North China Plain Based on Multi source Satellite Remote Sensing. *J. Remote Sens.* **2018**, *22*, 12.
63. Judd, L.M.; Al-Saadi, J.A.; Szykman, J.J.; Valin, L.C.; Janz, S.J.; Kowalewski, M.G.; Eskes, H.J.; Veefkind, J.P.; Cede, A.; Mueller, M. Evaluating Sentinel-5P TROPOMI tropospheric NO_2 column densities with airborne and Pandora spectrometers near New York City and Long Island Sound. *Atmos. Meas. Tech.* **2020**, *13*, 6113–6140. [CrossRef]
64. Dong, Z.; Gang, Z.; Zhong, L.; Yan, X.; Lan, Z.; CAS. Remote Sensing Monitoring of Tropospheric NO_2 Density in Chengdu-Chongqing Urban Agglomeration Based on OMI Data. *Resour. Environ. Yangtze Basin* **2019**, *28*, 2239–2250.

65. Lin, J.; Liu, M.; Xin, J.; Boersma, K.F.; Spurr, R.; Martin, R.; Zhang, Q. Influence of aerosols and surface reflectance on satellite NO_2 retrieval: Seasonal and spatial characteristics and implications for NOx emission constraints. *Atmos. Chem. Phys.* **2017**, *15*, 12653–12714.
66. Government, G.P.P.S. Guizhou Province's Three Year Action Plan for Winning the Blue Sky Defense War. Available online: https://www.guizhou.gov.cn/zwgk/zfgb/gzszfgb/201810/t20181017_70515165.html (accessed on 10 October 2024).
67. Shikwambana, L.; Mhangara, P.; Mbatha, N. Trend analysis and first time observations of sulphur dioxide and nitrogen dioxide in South Africa using TROPOMI/Sentinel-5P data. *Int. J. Appl. Earth Obs. Geoinf.* **2020**, *91*, 102130.
68. Li, F.; Ju, T.; Ma, C.; Xian, L. Research on Absorbent Aerosols in Gansu Province Based on Satellite Remote Sensing. *Chin. Environ. Sci.* **2019**, *39*, 11.
69. Peng, X.; Haiyan, S.; Qing, L.; Xuehai, F.; Chunhui, Z.; Kai, L.; Xianqin, W.; Aijiang, Y. Analysis of the Characteristics of Air Pollutant Concentration Changes and Air Mass Transport Sources in Guizhou Province. *J. Guizhou Univ. (Nat. Sci. Ed.)* **2023**, *40*, 101–111.
70. Zheng, Z.; Yang, Z.; Wu, Z.; Marinello, F. Spatial Variation of NO_2 and Its Impact Factors in China: An Application of Sentinel-5P Products. *Remote Sens.* **2019**, *11*, 1939. [CrossRef]
71. Lu, F.; Yuan, Y.; Hong, F.; Hao, L. Spatiotemporal variations and trends of air quality in major cities in Guizhou. *Front. Environ. Sci.* **2023**, *11*, 1254390. [CrossRef]
72. Zhou, C.; Li, Q.; Zhang, L.; Ma, P.; Chen, H.; Wang, Z. Remote sensing monitoring of spatiotemporal characteristics of NO_2 in China from 2005 to 2015 and analysis of influencing factors. *Remote Sens. Technol. Appl.* **2016**, *31*, 1190–1200.
73. Liu, X.; Yi, G.; Zhou, X.; Zhang, T.; Lan, Y.; Yu, D.; Wen, B.; Hu, J. Atmospheric NO_2 Distribution Characteristics and Influencing Factors in Yangtze River Economic Belt: Analysis of the NO_2 Product of TROPOMI/Sentinel-5P. *Atmosphere* **2021**, *12*, 1142. [CrossRef]
74. Chi, Y.; Fan, M.; Zhao, C.; Yang, Y.; Fan, H.; Yang, X.; Yang, J.; Tao, J. Machine learning-based estimation of ground-level NO_2 concentrations over China. *Sci. Total Environ.* **2022**, *807*, 150721. [CrossRef]
75. Guizhou Energy Administration. Guizhou Province Clean Energy Development "13th Five-Year Plan". Available online: https://www.guizhou.gov.cn/zwgk/zdlygk/jjgzlfz/ghjh/zxgh_5870292/201707/t20170726_62044036.html (accessed on 10 October 2024).
76. Guizhou Provincial People's Government. Action Plan for Comprehensive Control of Industrial Enterprise Atmospheric Pollution in Guizhou Province (2016–2020). Available online: https://www.guizhou.gov.cn/zwgk/zfgb/gzszfgb/201405/t20140506_70519599.html (accessed on 12 March 2023).
77. Standing Committee of the Guizhou Provincial People's Congress. Regulations on the Prevention and Control of Atmospheric Pollution in Guizhou Province. Available online: https://sthj.guizhou.gov.cn/zwgk/zdlyxx/fgybz/flfgjbz/201810/t20181029_76925218.html?isMobile=true (accessed on 10 October 2024).
78. Yang, Y. Temporal and Spatial Characteristics of Air Pollution in the Urban Area of Zunyi City and Analysis of Pollution Causes. Masters's Thesis, Guizhou University, Guiyang, China, 2022. [CrossRef]
79. Zunyi Municipal People's Government. Annual Implementation Plan for the Prevention and Control of Atmospheric Pollution in Zunyi City in 2017. Available online: https://www.zunyi.gov.cn/zwgk/zfwj/zfbf/201710/t20171025_68772391.html (accessed on 12 March 2023).
80. Zunyi Municipal People's Government. Three-Year Action Plan to Win the Battle for Blue Skies in Zunyi City. Available online: https://www.zunyi.gov.cn/ztzl/lszt/cjwmcs/cjdt/201812/t20181225_68747233.html (accessed on 10 October 2024).